Towards Thermo-reversible Pickering Emulsions

Master's Thesis
Van 't Hoff Laboratory for Physical and Colloid Chemistry

Utrecht, 2015

Author: Micah J.M. van der Vaart

Supervised by:

Chris H.J. Evers
Willem K. Kegel

Abstract

The stabilization of emulsions has been intensively studied and applied in e.g. food science. One method of stabilization is to cover the surface of droplets of oil in water by adsorbed colloidal particles in so-called Pickering emulsions. The stability of the emulsion is determined by the adsorption strength of the colloids, which is determined by the particle morphology, contact angle and the interfacial tension. This adsorption is usually irreversible and can usually be tuned by the size, shape and chemistry of the particle, now however, we propose a system with tunable interfacial tension. Therefore, we use binary mixtures with a closed-loop phase diagram and a thermally tunable interfacial tension, to obtain temperature-induced Pickering-like emulsions. A purpose-built heating set-up is designed to allow for a controllable uniform temperature. For two different binary mixtures, thermally tunable adsorption of colloids was obtained. Furthermore, at high temperatures a stable Pickering-like emulsion was induced. These temperature-induced Pickering-like emulsions are the first step towards thermo-reversible Pickering-like emulsions.

Contents

Chapter 1

Introduction

Liquid mixtures with partial miscibility allow us to study properties of an interface with easily tunable parameters. These mixtures have been extensively studied and used as model systems for modelling closed-loop phase behaviour or inducing colloidal attractions [1, 2, 3, 4]. In particular, mixtures exhibiting an immiscibility region that is completely surrounded by a miscibility region, so-called re-entrant mixtures show a closed loop in their phase diagram (fig. 2.2). These mixtures are of interest to study near-critical-point behaviour of fluids. Close to the critical point, phenomena such as attraction of colloids by critical Casimir forces [5] or critical contributions to the shear viscosity [6] arise.

Above the critical point, phase separation occurs, and temperature strongly influences the difference in the composition of the two phases. Consequently temperature can be used to tune interfacial properties such as the interfacial tension and wetting behaviour.

Phase separated droplets can be stabilized by adsorbed colloidal particles. Stabilization in this manner is called Pickering stabilization. The particles at the interface prevent the interfaces to touch, and the droplets to coalesce. Whereas often surfactant molecules are used to stabilize the interface, this method is surfactant-free. Pickering emulsions are widely used to stabilize emulsions and are of interest in for example food products, where for example starch particles are used as stabilizer [7].

In this report, we describe the behaviour of two binary mixtures with a closed immiscibility region in the phase diagram. We use a purpose-built heating set-up to be able to control the temperature while observing the system by optical microscopy. The demixing behaviour of the binary mixtures is described for temperatures just above the critical point. These mixtures were then used to obtain thermally tunable adsorption of colloids and temperature-induced Pickering-like emulsions, a first step towards thermo-reversible Pickering emulsions.

Chapter 2

Theory

2.1 Closed-loop phase behaviour binary mixtures

The supposed first case of a closed loop phase diagram was observed by Hudson [8] in 1904. The mixture was of nicotine and water, the form of the phase diagram stems from the nicotine being able to make more than one hydrogen bond with a water molecule, as further explained below. In the following years several more systems with such behaviour were discovered.

The miscibility properties of a mixture of fluids is governed by the interactions between the unlike species and the like species. The total energy is governed by competition between interaction energies and configurational entropy of unbound species. If the unfavourable interaction between unlike species is dominant over the entropy, the fluids will separate in two phases each rich in one of the species. For most mixtures, at higher temperatures thermal fluctuations will dominate over the interaction energy and the two phases will mix. More complex behaviour is observed for systems with anisotropic interactions and/or interactions that vary with parameters such as temperature, such as hydrogen bonds.

The closed-loop phase behaviour is due to directional bonds, such as hydrogen bonds, between the two liquids [9]. Brovchenko and Oleinikova propose a model describing the phase diagram based on the number of bonds a water molecule makes with a pyridine molecule [10]. They describe three different states: the 0H state, with no hydrogen bonds between water and pyridine, the 1H state, with one hydrogen bond between the water molecule and the nitrogen atom, and the 2H state wherein the π system of the pyridine forms a second hydrogen bond with the water molecule. The 1H state allows the water molecule to bind with other water molecules, creating a shell of water around the pyridine, stabilizing the molecule. The 0H and the 2H state promote demixing, in the 0H state, molecules have more freedom of movement and the higher entropy dominates. Due to the two bonds in the 2H state, this state is dominated by an increased total bond energy. At high temperatures the thermal energy allows for breaking of hydrogen bonds, so that the 0H state dominates. At low temperatures the 2H state dominates due to lower entropy. At intermediate temperatures the 1H state dominates and allows for miscibility. This model accurately describes the behaviour of binary mixtures and the dependence on the hydrogen bond strength (fig. 2.1).

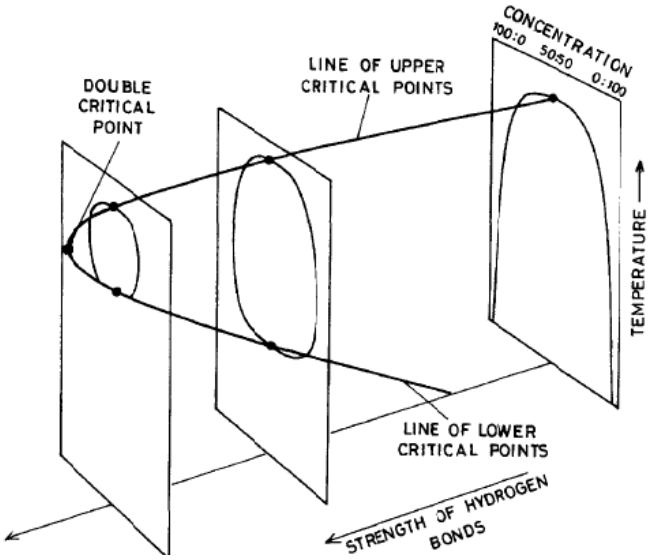

Figure 2.1: Dependence of the phase diagram of a binary mixture on the strength of the hydrogen bonds between the two species. At high bond strength, a lower critical point appears above the freezing point of the mixture. Therefore a system at higher hydrogen bond strength will show re-entrant phase behaviour [11].

Several of these binary mixtures are often studied, foremost the quasi-binary mixture of 3-methylpyridine (3MP) with H_2O and D_2O. In this mixture, the ratio of normal and heavy water is used to tune the hydrogen bond strength [12]. Re-entrant phase transitions can also be observed in some binary gas mixtures, liquid crystal systems, gels and some magnetic systems [11].

The properties of these mixtures are interesting because temperature serves as a direct control for many properties of the system. At temperatures just below the critical point, mesoscale inhomogeneities arise and concentration fluctuations act over longer lengths [13].

Above the critical point, temperature influences the difference in the composition of the two phases (see fig. 2.2). Therefore temperature can be used to tune interface properties such as the interfacial tension and wetting behaviour.

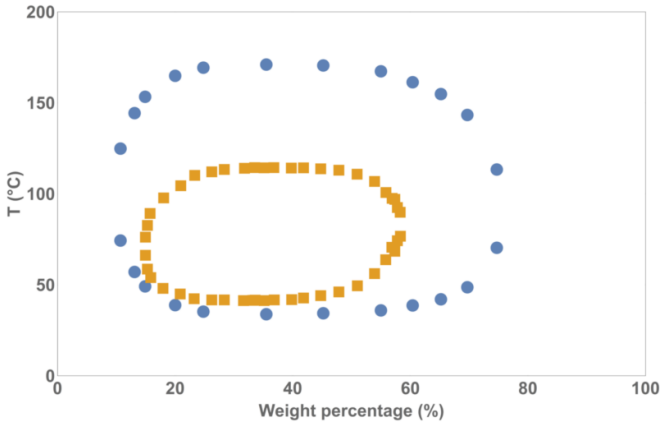

Figure 2.2: Phase diagrams of the two studied systems. The yellow squares represent 3-methylpyridine in D_2O [9] and the blue dots 1-propoxy-2-propanol in H_2O [14]. Both show an asymmetric closed loop.

The interfacial tension determines the contact angle of the interface with for instance glass. The three interfacial tensions enact force on the contact line and together lead to certain contact angle (see fig. 2.3), as described by Young's equation:

$$\gamma_{\mathrm{SB}} - \gamma_{\mathrm{SA}} - \gamma_{\mathrm{AB}} \cos\theta_{\mathrm{c}} = 0. \tag{2.1}$$

In which the three interfacial tensions, γ_{SB} between substrate (S) and continuous phase (B), γ_{SA} between the substrate and the droplet phase (A), and, γ_{AB} between the droplet and the continuous phase, determine the contact angle θ_{c}.

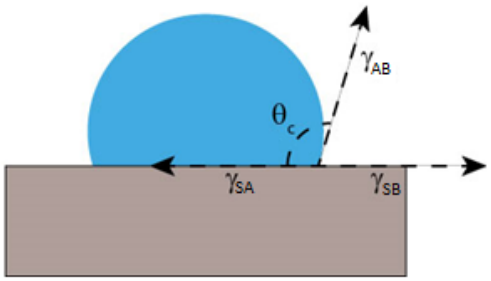

Figure 2.3: Schematic representation of the Young contact angle as determined by the three interfacial tensions. In blue is a droplet of liquid on the, in grey, substrate

Two different radii can be defined as shown in fig. 2.4. The radius of the droplet itself , R_{droplet}, and the radius of the contact ring with the substrate, R_{glass}. The ratio between these two radii depends on the contact angle, θ_{c}, of the droplet with the glass, following:

$$R_{\text{glass}}/R_{\text{droplet}} = \cos(\theta_c - 90°). \tag{2.2}$$

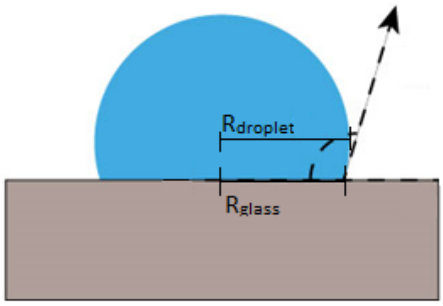

Figure 2.4: Schematic representation of the two different observable radii of a droplet on a substrate. In blue is a droplet of liquid on the, in grey, substrate

2.2 Colloidal adsorption and Pickering emulsions

The adsorption of a colloid on an interface depends on several parameters, mainly the size of the particle, R, the contact angle between colloid and interface, θ_c, and the interfacial tension, γ. The energy of adsorption can be described for spherical colloids by a fairly simple formula [15]:

$$E = \pi R^2 \gamma (1 \pm \cos\theta_c)^2. \tag{2.3}$$

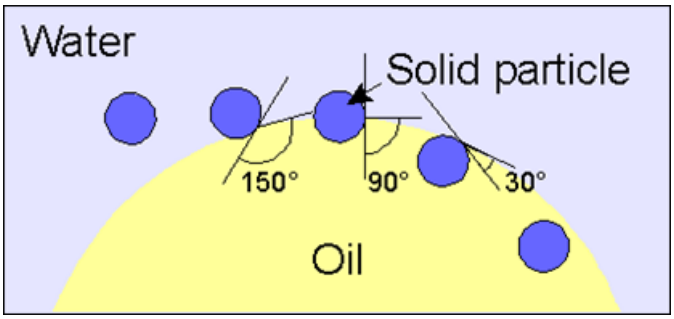

Figure 2.5: A schematic representation of a particle adsorbed to a droplet at different angles [16].

For a similar system to the ones studied in this thesis, with a phase diagram similar to that of 3MP and PnP, of 2,6 lutidine/H_2O, the interfacial tension is about $10^{-2}\,\text{mN}\,\text{m}^{-1}$ at $\Delta T = 0.1\,°\text{C}$ (see fig. 2.6) [17], assuming a contact angle between 45° and 135° for a 1 µm particle, this leads to adsorption energies on the order of $5 \times 10^2\,\text{k}T$.

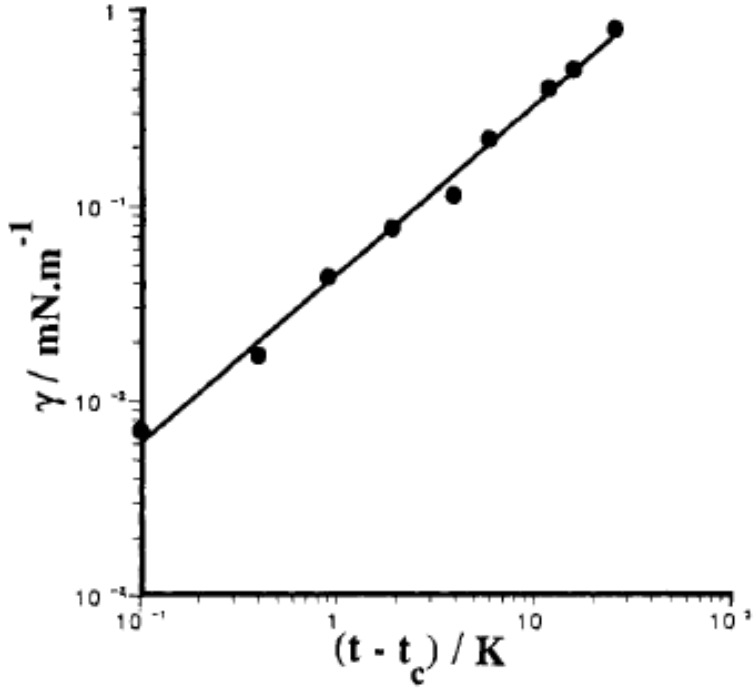

Figure 2.6: Dependence of the interfacial tension on the temperature, t, compared to the critical temperature, t_c, for a binary mixture of 2,6-lutidine and water as measured by Grattoni et al. [17].

If the surface of a droplet is sufficiently covered by particles, droplets are prevented from coalescing by the repulsion, such as excluded volume or electrostatic repulsion, of the particles. This is a so-called Pickering emulsion. The stabilization is strongest when the wetting angle of the particles is close to 90°.

2.3 Peltier heating

Peltier heating is a thermo-electric effect discovered by Jean Charles Athanase Peltier in 1834, and is the counterpart of the earlier discovered Seebeck effect in 1821. The Seebeck effect describes how a current can be generated by a junction of two different conductors in a temperature gradient [18]. A good example of the use of this is in thermocouples, where the temperature defines the voltage generated by the junction. Peltier discovered that if a current is applied to such a junction the heating produced was more than just resistive, Joule, heating [19]. When current was made to flow through the junction heat transfer took place from one side to the other. A schematic representation of such a junction is shown in fig. 2.7.

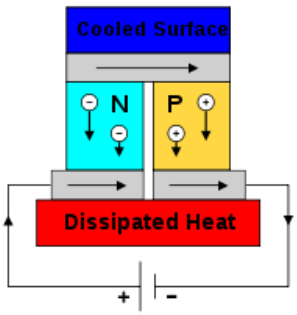

Figure 2.7: A schematic representation of a Peltier junction.

This heat transfer per unit time, $\dot{Q}$, is equal to:

$$\dot{Q} = (\Pi_A - \Pi_B)I. \tag{2.4}$$

In which Π_A and Π_B are the Peltier coefficients of both conductors, and I is the current. Total heating is a combination of this Peltier heating, Joule heating and thermal gradient effects.

Commonly different doped semiconductors are used for the junction. The heating can be improved by stacking multiple junctions on top of each other.

Chapter 3

Materials & Methods

3.1 Binary mixtures

Two different binary mixtures were used. One consisting of 3-methylpyridine (3MP) ($\geq 99.5\,\%$, Aldrich) and D_2O (99.9 %, Sigma Aldrich) with critical temperature $T_c \approx 39\,°C$ at approximately 31.5 wt% 3MP (fig. 2.2). The other consisted of 1-propoxy-2-propanol (PnP) (99 %, Aldrich) and Milli-Q H_2O (Synergy Millipore purifier) with $T_c \approx 31\,°C$ at approximately 40 wt% PnP (fig. 2.2).

3.2 Microscopy set-up

Two different microscopy set-ups were used, a commercially available heating stage for diascopic microscopy, and a purpose-built set-up using a Peltier element for episcopic microscopy. Furthermore two different sample cells were used.

3.2.1 Diascopic microscopy

In diascopic microscopy the sample is illuminated by a light source above the sample and the image captured via the objective with a camera below the sample. A commercially available, Linkam heating stage with a Linkam TP 93 controller, was used in conjunction with a Nikon TiU inverted microscope. This stage allowed for precise heating to a desired temperature and and with a precise rate of heating, but because it consisted of a circular heating element with a hole in it, temperature gradients in the x,y plane were unavoidable. The circular hole allowed for light to pass through the sample enabling diascopic microscopy.

3.2.2 Episcopic microscopy

In order to avoid the temperature gradient in the x,y plane a set-up was purpose-built to uniformly heat a sample. For temperature control a Peltier heating element was chosen, a PELTIER-ELEMENT QC-18-0.6-1.2M element in conjunction with a QC-PC-CO-CH1 controller supplied by

Quick-Cool, attached to a metal block that acts as a heat reservoir. Temperature control using the controller tended to overshoot or undershoot the desired temperature, afterwards the temperature would oscillate around the set temperature. Better temperature control was achieved by placing a stepwise variable resistor between the element and the current source, allowing regulation of the current by varying the resistance. Since the heat transfer is linearly dependent on the current (seesection 2.3), this allowed intuitive temperature control. A temperature probe, delivered together with the controller, was placed on the heat reservoir just next to the element and was read out using the controller. This set-up allowed for precise and constant temperature control, within 0.1 °C, even when the sample was placed on the microscope.

Because the heat reservoir was placed on top of the sample, diascopic microscopy was impossible, but episcopic microscopy still worked fine. In episcopic microscopy the sample is illuminated through the microscope objective and the reflected light is captured on the camera. This set-up was used in conjunction with a motorized Ti-E Nikon inverted microscope.

Using either method the temperature of the mixture itself was not measured. Instead, the temperature of either the heat reservoir block or the heating stage was measured and is reported in this thesis as the relative temperature $\Delta T = T - T_c$. The placement of the temperature probe on the block caused the displayed temperature to be off during fast heating and cooling, but accurate after a short equilibration time, especially in the episcopic set-up. The temperature of the block at the critical point agreed well with expected critical temperatures in each sample, being off by 0.5 °C at most. Therefore, ΔT could be reported quite accurately.

3.2.3 Sample cell

All reported measurements were carried out in a glass capillary attached to a glass plate. Capillaries were 0.05 µm × 50 µm × 1000 µm glass capillaries (Vitrotubes # 5005-050) unless otherwise stated. The capillaries were sealed in a flame and glued ( )shut to prevent evaporation.

To increase the resolution, a different sample set-up was tried, consisting of a, glued together, cell with an optical glass window covering a droplet held between spacers as shown schematically in fig. 3.1.

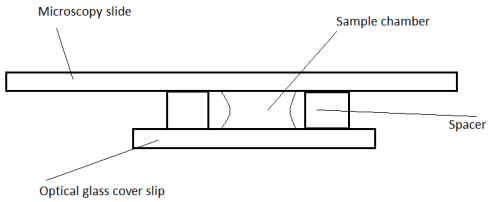

Figure 3.1: Schematic representation of the optical window sample cell. This sample cell can be illuminated from above in our diascopic set-up or from below in the episcopic set-up, with the heating reservoir on top of the microscopy slide.

Two separate modifications were made to this sample cell, to make the surface hydrophobic. The first method was to cover the microscopy slide with a sheet of hydrophobic Teflon (0.05 mm thick, supplied by Bola). The other method was to functionalize the microscopy slide and the cover

slip with a hydrophobic end group. Functionalization was performed using hexamethyldisilazane (HMDS) (ReagentPlus, 99.9 %, Aldrich), following the procedure of Prucker et al. [20]. The microscopy slide and cover slip were placed in a closed container with some droplets of HMDS and heated overnight in an oven at 80 °C. At this temperature the HMDS evaporates and the vapour reacts with the glass, covalently binding the HDMS to the surface of the glass [21].

3.3 Microscopy image analysis

To determine the contact angle between the droplet and the surface, pictures were made using diascopic microscopy focusing on the middle of the droplet. At this focus level both the droplet radius and the contact ring between droplet and surface, were clearly visible. Radii were measured manually using a three point technique for circle recognition (using ITEM) for each temperature. This was done for multiple droplets of different sizes. Measured radii were then used to determine the contact angle following eq. (2.2).

To measure the retention time of polystyrene colloids on the droplet interface, a capillary containing a mixture of PnP and H_2O with 40 wt% was heated with the episcopic set-up to $\Delta T = 0.5\,°C$. A time series was taken at three different heights to allow for particle tracking in three dimensions. The particles were tracked by eye to measure the retention time. Reported retention times are the difference between the time stamps of the image just before and just after the particle being adsorbed to the interface.

3.4 Colloids

Polystyrene spheres were previously prepared by Chris Evers [22], using divinylbenzene as crosslinker, and potassium persulfate as an initiator. Particles were washed three times after synthesis and dispersed in Milli-Q water. The synthesis is surfactant-free.

Cross-linked poly(styrene-*co*-acrylic acid) spheres were previously prepared by emulsifier-free polymerization of styrene, acrylic acid and divinyl benzene under nitrogen flow, using potassium persulfate as an initiator, by Chris Evers [22]. Particles were then washed three times and dispersed in Milli-Q water.

3.4.1 Preparation of fluorescent colloids

Two approaches were taken to obtain fluorescent colloids. One approach was to swell the polystyrene particles with dye, and the other to covalently attach dye molecules to functionalised polystyrene seed particles.

Dye incorporated by swelling

To prepare non-covalent bound dyed PS colloids, a method by Daniela Kraft was used [23]. A fluorescent dye, Rhodamin B, is added, dissolved in a swelling agent, dichloromethane. As the dichloromethane diffuses inside the particles together with the dye, the particles swell. After evaporation of the dichloromethane, the dye is left behind, incorporated in the particles. 5 µl

of 1 mM Rhodamin B solution in dichloromethane was added to 50 µl of the 50 times diluted colloid dispersion and kept on a rolling bank for 4 days. The dichloromethane was then left to evaporate for 6 hours.

Covalently bound dye

To synthesize fluorescein labeled colloids, functionalized polystyrene particles previously prepared by Frans Dekker were used [24]. They were polystyrene (PS) colloids with a diameter of about 300 nm functionalised with a 2-hydroxyethyl acrylatebromine (HEA) polymer brush, ending in a co-polymer block of HEA and glycidyl methacrylate (GMA). This GMA contains an epoxide group that can react to primary amines.

250 µl dispersion in water was washed three times with dimethylformamide (DMF) and then transferred to DMF. The dispersion was transferred to a reaction tube and placed in an oil bath. The set-up was wrapped in aluminium foil to keep out light, protecting the fluorescent groups. To the dispersion, 250 µl fluoresceinamine solution in DMF was added ($0.3\,\mathrm{mg\,ml^{-1}}$).The solution was then heated to 60 °C and stirred with a magnetic bar for 24 h.

After 24 hours the oil bath was shut off. The dispersion was light salmon pink. The dispersion was then washed three times with DMF and three times with Milli-Q water. After the last washing step the colloids were re-dispersed in 1 ml Milli-Q water. During washing steps it was apparent that some fluoresceinamine had not reacted due to the yellowish colour of the supernatant. After the final washing step the supernatant was a clear colourless liquid.

Chapter 4

Results & Discussion

4.1 Sample Cell

Two types of sample cells were tested: a flame and glue sealed capillary, and a glued cell with an optical glass window. When the sample was in contact with the glue large, possibly glue, particles were observed.

Thin capillaries were used with a thickness of 0.5 µm, because they could be heated uniformly in the x, y plane, although it also possibly led to sharper temperature gradients in the z direction. The disadvantage of capillaries is a reduced resolution because the capillaries were not made from optical glass.

The sample cell with an optical glass window was, however, less successful. Upon applying a droplet of PnP/H_2O or 3MP/D_2O on a microscopy slide and covering it with a cover slip, the droplet completely wetted the glass and leaked out at the edges.

To prevent this wetting, the substrate was covered with a thin sheet of Teflon, or functionalised with HDMS. Using a Teflon sheet, the resulting surface was not completely flat. Hence the droplet got in contact with the edges and leaked out. To obtain a flat surface, coating the substrate with HDMS was successful, as the contact angle of a droplet of water on the surface, determined by eye, was significantly larger than for an untreated glass slide. Applying a droplet of the binary mixture on the substrate led to a stable droplet. Even after placing and applying pressure on the cover slip the droplet remained in place, and did not leak out. Upon heating the sample though, the droplet started wetting the glass substrate and quickly escaped underneath the spacers. This behaviour is likely caused because the temperature increases the strength of hydrophobic interactions in the mixture. This increase does not only cause the demixing, it also changes the wetting properties, such that the sample wets the hydrophobic surface.

Because neither a hydrophobic nor a hydrophilic substrate will allow for a stable droplet at all temperatures, for further measurements capillaries were used.

4.2 Demixing

Upon gradually heating mixtures of 3MP/D_2O or PnP/H_2O above the critical temperature, phase separation occurs as can be seen in figs. 4.1 and 4.2. First, droplets nucleate (fig. 4.1a), and, if kept at a steady temperature, coalescence and Ostwald ripening lead to polydisperse large droplets (fig. 4.1b). If kept at a steady temperature sufficiently long, the sample macroscopically phase separated in a water-rich and a water-poor phase.

At temperatures very close to the critical temperature, T_c, the interface becomes vague (see fig. 4.2), and the time it takes for droplets to reform their spherical shape after coalescence increased to a minute or more (see fig. 4.3). The loss of spherical shape and the fading of the interface near the critical point indicate that the interfacial tension gets really low. However, the process of reforming is also slowed by pinning of the interface to the glass.

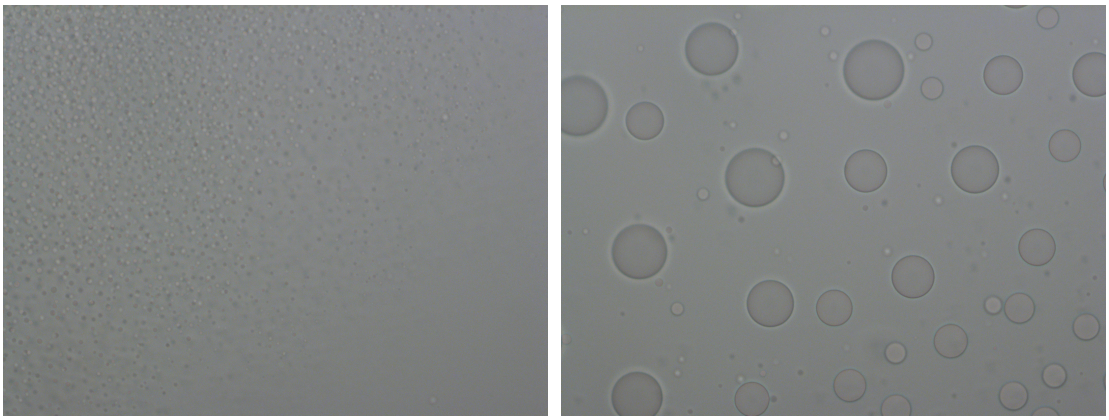

(a) (b)

Figure 4.1: Diascopic microscopy images of demixing behaviour of a 34.4 wt% 3MP/D_2O mixture. After heating above the critical temperature, small droplets appear (a) that in time coalesce into larger droplets (b).

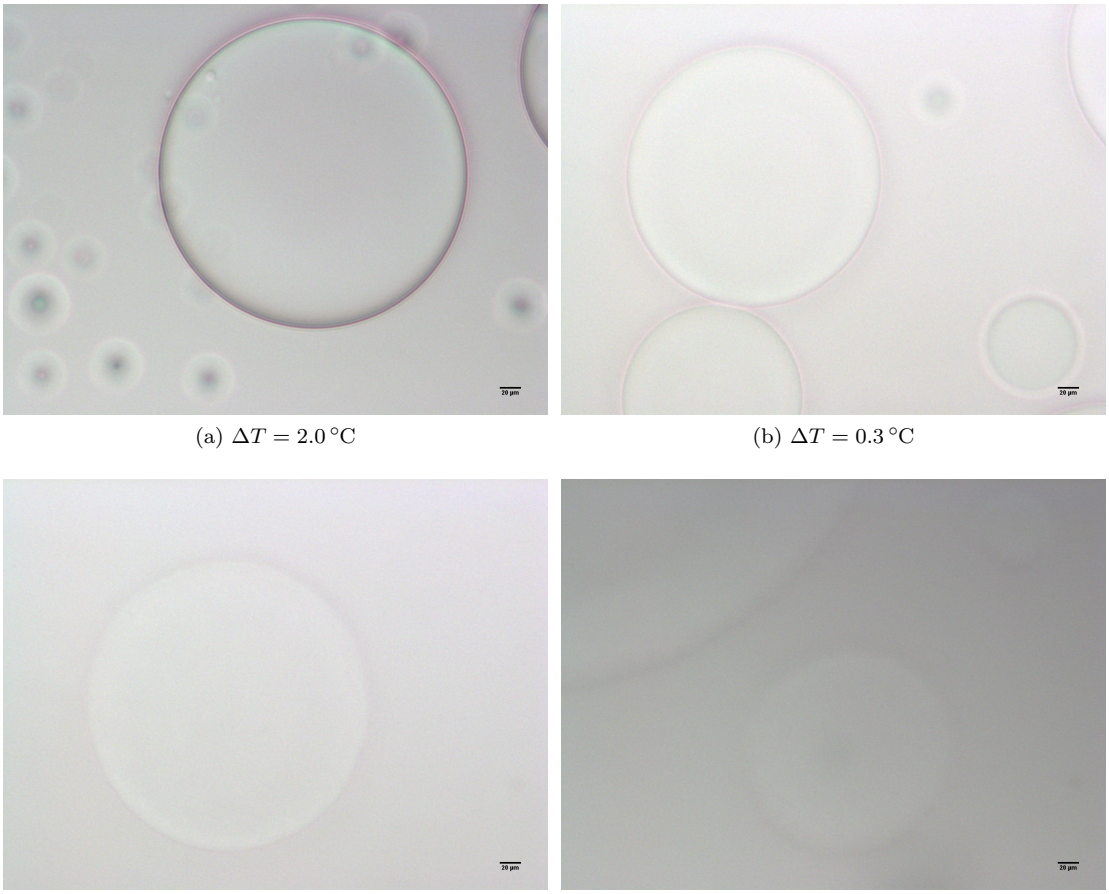

(a) $\Delta T = 2.0\,^{\circ}\mathrm{C}$ (b) $\Delta T = 0.3\,^{\circ}\mathrm{C}$

(c) $\Delta T = 0.2\,^{\circ}\mathrm{C}$ (d) $\Delta T = 0.1\,^{\circ}\mathrm{C}$

Figure 4.2: Diascopic microscopy images of demixing behaviour of a 39 wt% PnP/H_2O mixture. At high ΔT the interface is sharp and clear (a). Close to the critical temperature (b)-(d) the interface becomes more diffuse and fades out.

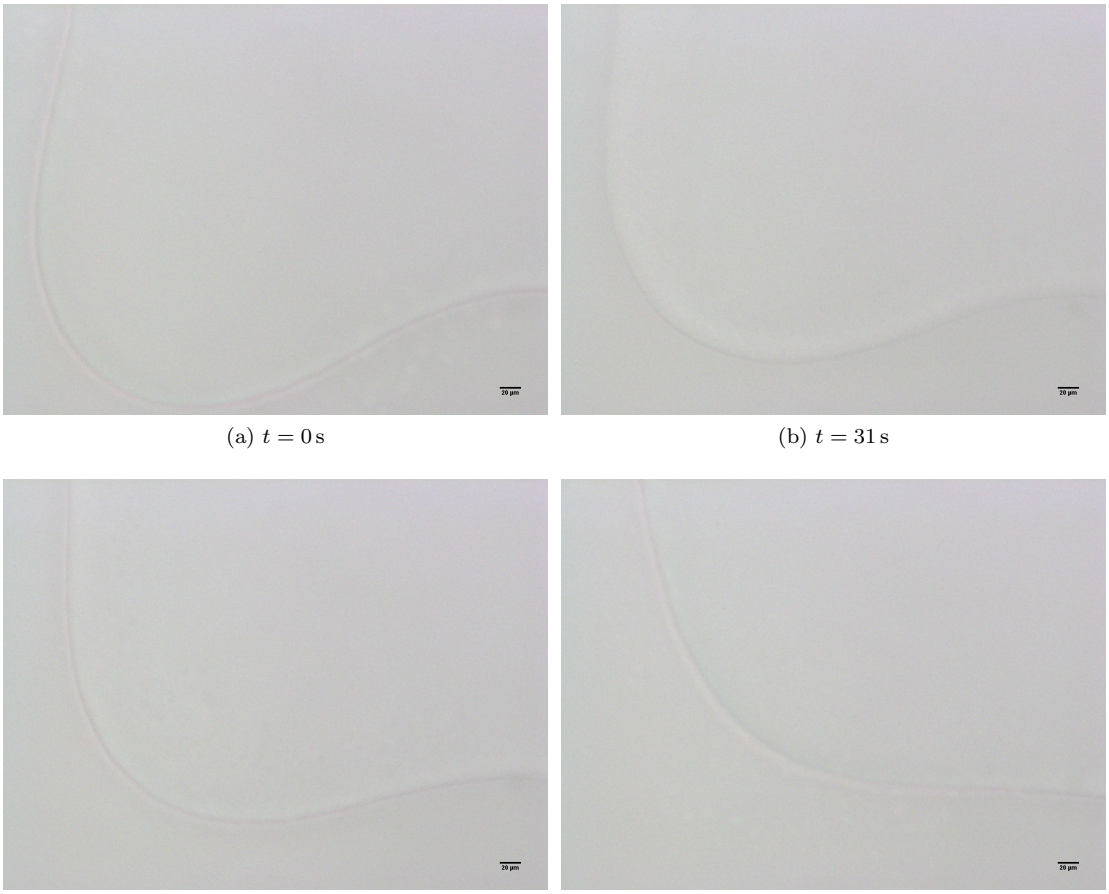

(a) $t = 0\,\mathrm{s}$ (b) $t = 31\,\mathrm{s}$

(c) $t = 49\,\mathrm{s}$ (d) $t = 95\,\mathrm{s}$

Figure 4.3: Diascopic microscopy time series of a two droplets coalescing in a 39 wt% PnP/H_2O mixture at $\Delta T = 0.2\,°\mathrm{C}$. Due to the low interfacial tension coalescence is very slow.

Due to the fact that the composition of the two phases is dependent on temperature (fig. 2.2), the interfacial tension depends on the temperature, and thus the contact angle, θ_c depends on temperature as well. In fig. 4.4, the experimentally determined contact angle is plotted against the temperature, showing a clear decrease of the contact angle upon increasing temperature. The hysteresis shown is to be expected because of pinning, however, the hysteresis does fall within the error of measurement. For the later measurements in the series, only a few droplets could be measured, due to coalescence of the droplets. The contact angle was measured from microscopy images, comparing the size of the droplet radius and the contact radius, as described in section 3.3.

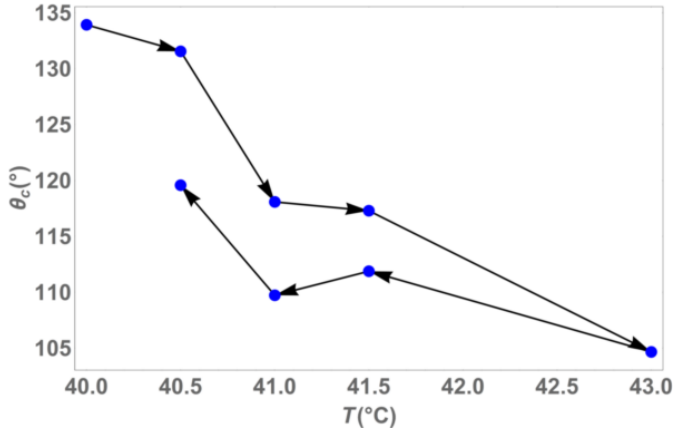

Figure 4.4: The contact angle, θ_c, as a function of the temperature for a 31.4 wt% 3MP/D_2O mixture. Arrows indicate the direction of measurement.

Upon increasing the temperature, the composition of both phases becomes more different and the contact angle, θ_c, decreases, approaching 90°. Rewriting Young's equation gives:

$$\theta_c = \cos^{-1}(\frac{\gamma_{SA} - \gamma_{SB}}{\gamma_{AB}}). \tag{4.1}$$

At higher T, the measured θ_c decreases. Hence, either the difference between the interfacial tensions of either phase with the wall, $\gamma_{SA} - \gamma_{SB}$, decreases, or the interfacial tension between the two phases, γ_{AB}, increases. Since the compositions of the two phases become more different upon increased temperature, it is expected that γ_{SA} and γ_{SB} diverge, and that $\gamma_{SA} - \gamma_{SB}$ increases instead of decreases. However, an increase of γ_{AB}, is exactly what we expect. Hence, the increase of the contact angle with temperature illustrates that the interfacial tension can be significantly tuned with temperature.

4.3 Temperature-controlled interface adsorption

The next step towards a temperature-induced Pickering emulsion is to thermally tune the adsorption of particles to the interface. Therefore polystyrene (PS) particles were studied in the binary mixtures at different temperatures above the critical point. This is shown in figs. 4.5 and 4.6. By increasing the temperature above a threshold value, $\Delta T \approx 2\,°C$, colloids seem to adsorb to the interface. This process is reversible and observed in both the 3MP/D_2O and PnP/H_2O mixture.

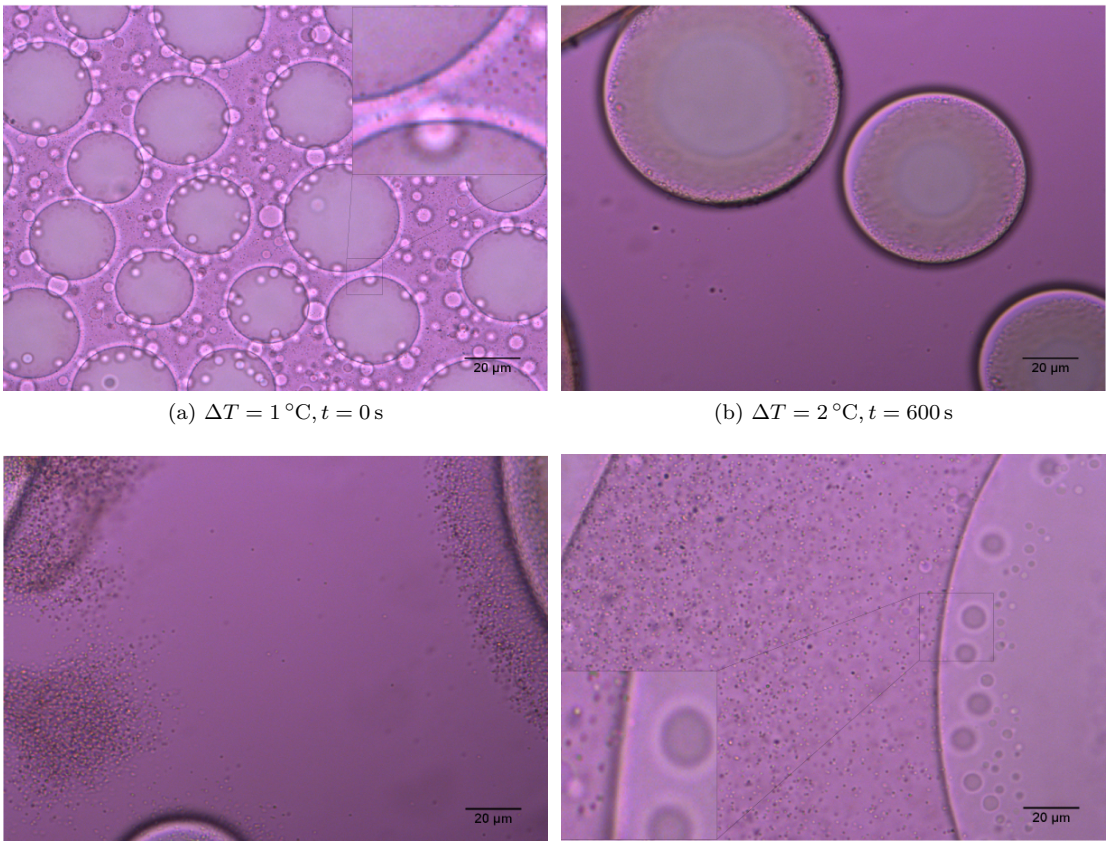

(a) $\Delta T = 1\,°\mathrm{C}, t = 0\,\mathrm{s}$ (b) $\Delta T = 2\,°\mathrm{C}, t = 600\,\mathrm{s}$

(c) $\Delta T = 1\,°\mathrm{C}, t = 670\,\mathrm{s}$ (d) $\Delta T = 0.1\,°\mathrm{C}, t = 1390\,\mathrm{s}$

Figure 4.5: Diascopic microscopy images of a mixture of 28.9 wt% 3MP and D_2O with polystyrene colloids and dyed with Rhodamine B. At $\Delta T = 1\,°\mathrm{C}$ (a) most colloids are in the continuous phase and only a few particles seem temporarily adsorbed to the interface. After heating to $\Delta T = 2\,°\mathrm{C}$ (b), almost all colloids are at the interface, while upon cooling back to $\Delta T = 1\,°\mathrm{C}$, the particles move away from the interface (c) and eventually, at $\Delta T = 0.1\,°\mathrm{C}$, are uniformly distributed in the continuous, water-rich, medium (d). The sample was heated and cooled at $1\,°\mathrm{C\,min^{-1}}$.

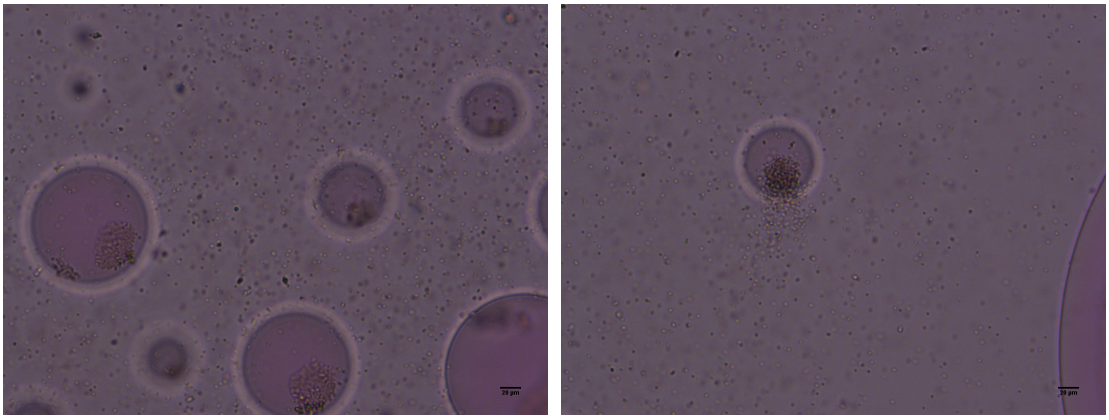

(a) $\Delta T = 2.2\,^{\circ}\mathrm{C}, t = 0\,\mathrm{s}$ (b) $\Delta T = 1.3\,^{\circ}\mathrm{C}, t = 200\,\mathrm{s}$

Figure 4.6: Diascopic microscopy images of a phase separated, Rhodamin B dyed, mixture of 40.4 wt% PnP and H_2O with polystyrene colloids. (a) At $\Delta T = 2.2\,^{\circ}\mathrm{C}$, colloids adsorb tightly to the interface between both phases. (b) Upon decreasing the temperature to $\Delta T = 1.3\,^{\circ}\mathrm{C}$, the colloids move away from the interface and diffuse back in to the continuous water-rich phase.

At ΔT close to zero, the particles all remain in the continuous, water-rich, phase with no particles found inside the droplets, some temporarily reside at the interface.

In both the 3MP/D_2O and the PnP/H_2O mixture, if the temperature is increased above $\Delta T = 2\,^{\circ}\mathrm{C}$, the colloids adsorb permanently to the interface. It seems that the surface tension gives rise to such adsorption energies that adsorption is favourable over the entropy gained from particles moving free in the continuous phase. This is observed for both mixtures as expected. However, for PnP/H_2O only a fraction of the colloids adsorb, while for 3MP/D_2O all particles adsorb. The origin of this difference is unknown, but could be of great significance. Wetting differences or difference in charges on the interface could play a role in this.

In both cases, if ΔT is decreased below the threshold value, all colloids detach from the interface and move back to the continuous phase.

As seen in figs. 4.5 and 4.6, particles attached to the interface float at the top of the droplet. In fig. 4.5, the droplet touches the top glass wall and because of this the colloids form a ring-like structure (fig. 4.7, left). In fig. 4.6, the droplets are attached to the bottom glass wall and thus the colloids form *islands* on top of the droplet (fig. 4.7, right). These islands move as a single entity, without any lone particles observed at the interface. This is an indication that there is attraction between the colloids on the interface. At detachment of the colloids in fig. 4.6 (b), the particles diffuse in one direction. This could be due to either a temperature gradient causing thermophoresis, or asymmetric 'evaporation' of the droplet.

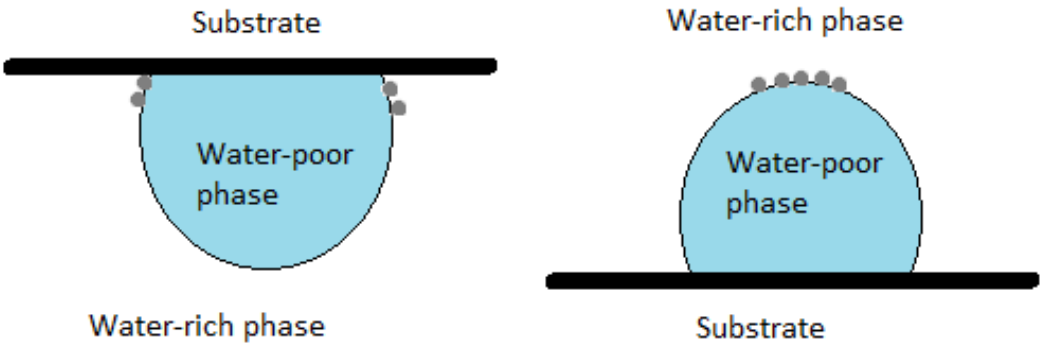

Figure 4.7: Schematic representation of droplets (light blue) attached to the glass (thick black line) with colloids (grey) gathered at the top. Left shows a droplet attached to the top glass wall, here colloids form a ring near the contact line between the droplet and the substrate, as in fig. 4.6. Right shows a droplet attached to the bottom glass wall, here colloids form an *island* on top of the droplet, as in fig. 4.5.

However, the energies reported in section 2.2 for a similar system are inconsistent with assuming that the decrease in interfacial tension causes desorption. Another possible explanation could be pinning, wetting or that the particles are not attached to the interface, but a driving force keeps them in close proximity. Possible causes of this driving force could be a charge on the interface or a concentration gradient close to the interface.

A macroscopically separated system was also studied using fluorescence microscopy, with Rhodamin B added as a dye, as shown in fig. 4.8. Figure 4.8 shows the advantage of using a dye with a preference for one of the phases, enhancing the contrast of the image. However, particles moved as a cluster in a toroidal flow near the interface, going from top to bottom. This made observation of the adsorption of single particles impossible.

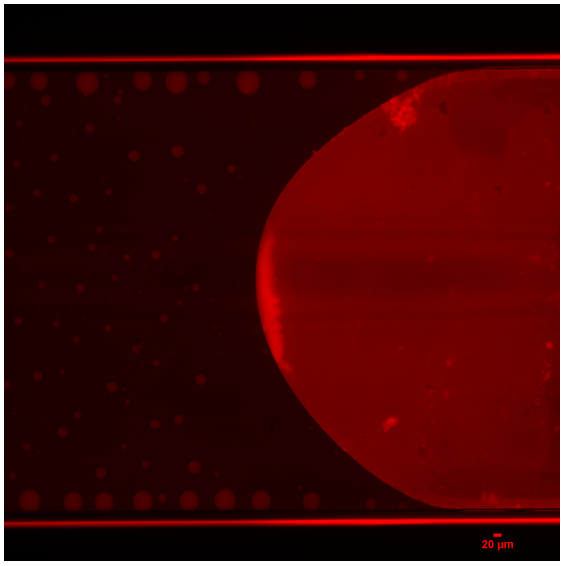

Figure 4.8: Episcopic fluorescence microscopy picture of a phase separated mixture of PnP and H_2O with PS colloids. Rhodamin B dye is responsible for the fluorescence. Particles are attached at the macroscopic interface. Due to a high local concentration of particles and a strong toroidal flow of particles near the interface, going from bottom to top, determining the adsorption of single particles is impossible.

4.4 Retention time

In both mixtures, two regimes can be identified. The first regime above $\Delta T \approx 2\,^{\circ}\mathrm{C}$ where colloids attach to the interface and stay there for longer than experimental rime scales, indicating that the adsorption energy seems to be a lot higher than kT. In the second regime from $\Delta T = 0\,^{\circ}\mathrm{C}$ to $2\,^{\circ}\mathrm{C}$, most colloids remain in the continuous phase, indicating low adsorption energies. Particles move to the interface and reside there temporarily, but this process is reversible (see fig. 4.9). At a temperature of $\Delta T = 0.5\,^{\circ}\mathrm{C}$, residence time was measured for 48 occasions of a particle residing temporarily at the interface and plotted in fig. 4.10.

The normalized histogram was fitted with an exponential function giving a characteristic retention time of 2.8 s. This indicates that the energy of adsorption is on the order of the thermal energy. Grattoni et al. report, for a binary mixture of 2,6-lutidine and water, an interfacial tension of $2 \times 10^{-2}\,\mathrm{mN\,m^{-1}}$, $0.5\,^{\circ}\mathrm{C}$ above T_c [17] (see fig. 2.6). Assuming a contact angle of 90° would give an adsorption energy of approximately $10^3\,\mathrm{k}T$ in our system (eq. (2.3)). This means that either the interfacial tension is hyper-low, or another effect is responsible for the short residence time of the particle. These effects could be distortion of the interface or a low contact angle of the particle with the interface, or the aforementioned possibility that particles are not attached at all. Unfortunately our experiments did not allow us to investigate these effects precisely, and more experiments are needed.

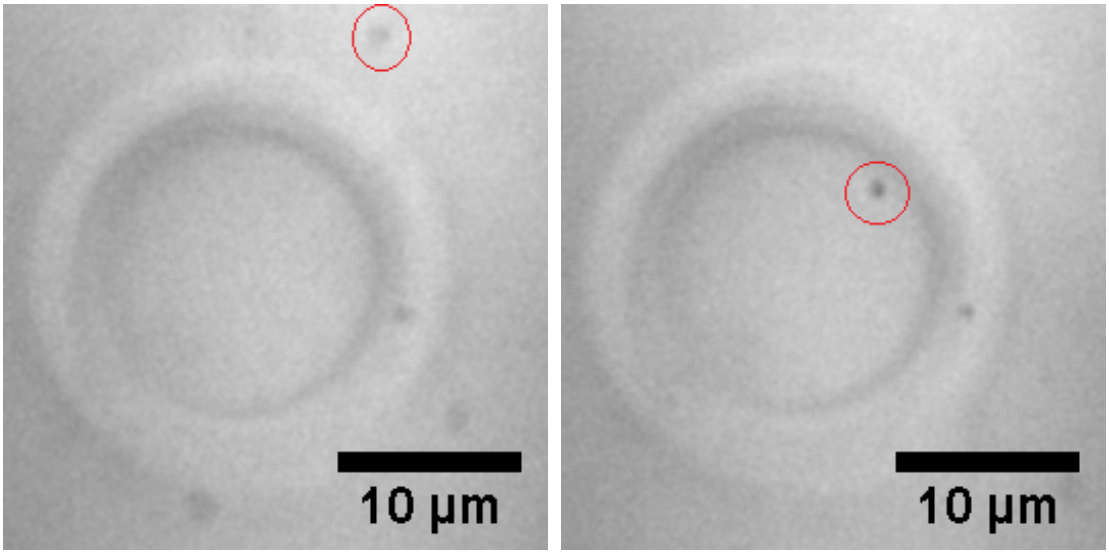

(a) $t = 0\,\mathrm{s}$ (b) $t = 2.01\,\mathrm{s}$

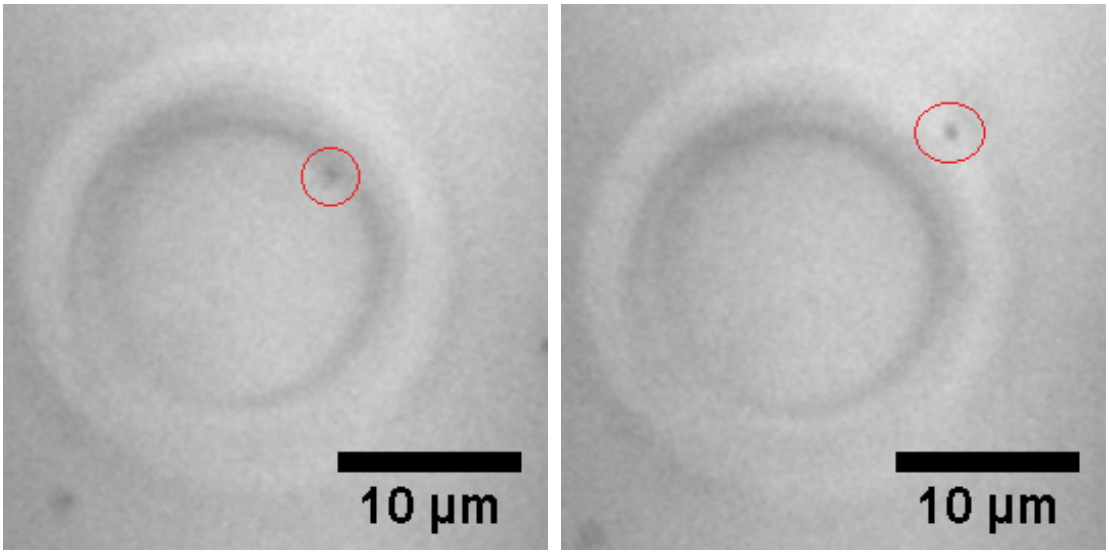

(c) $t = 5.97\,\mathrm{s}$ (d) $t = 8.01\,\mathrm{s}$

Figure 4.9: Episcopic microscopy images of the retention time measurement of a mixture of 39.7 wt% PnP/H_2O at $\Delta T = 0.5\,°\mathrm{C}$. a) First the particle is free, b,c) next the particle resides at or near the interface, d) finally the particle moves away from the interface.

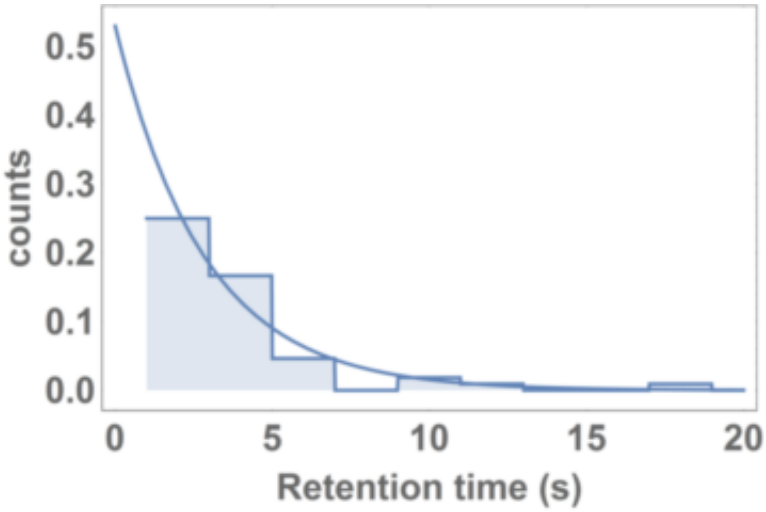

Figure 4.10: Normalized histogram of the retention times of PS colloids on the interface between the PnP and H_2O rich phases at $\Delta T = 0.5\,°C$. The line is an exponential fit of the data.

4.5 Pickering-like emulsion stabilization

The temperature-induced adsorption of colloids is used to try to obtain thermo-reversible Pickering stabilized emulsions. We studied a binary mixture with a high colloid concentration, the high concentration allowed for full coverage of the droplets at sufficiently high temperatures (fig. 4.11(b)). This full coverage of particles prevents coalescence of droplets, stabilizing the emulsion. Droplets in the Pickering stabilized state did not coalesce even when touching. Upon cooling, movement of the colloids increased and the particles detached from the interface, allowing the droplets to coalesce (fig. 4.11(c)). In accordance with the phase diagram (fig. 2.2) the amount of dispersed phase decreased and the droplets shrank. The highly concentrated cloud of detached colloids irreversibly agglomerated or adhered to the glass wall. Presumably being pushed together by flow or the shrinking droplets. Particles attached to the wall would only detach if the sample was cooled under T=28 °C but agglomerates would remain. Hence this process was not reversible.

In some cases the shrinking of the particle covered droplets led to the formation of colloidosome like aggregates as shown in fig. 4.12. As the temperature decreases the total amount of dispersed phase decreases (see fig. 2.2), thus the droplets shrink. The particles attached to the shrinking interface get pushed together and form a tight shell. By rapidly increasing the temperature followed by cooling of a binary mixture with high particle concentration, we provide a simple one-step procedure to create colloidosomes without the necessity of high shear. However, polydispersity of the colloidosomes is high, their number is low, and most of them are not complete. This process could possibly be improved by tuning colloid concentration, binary mixture composition and the rate of heating and/or cooling.

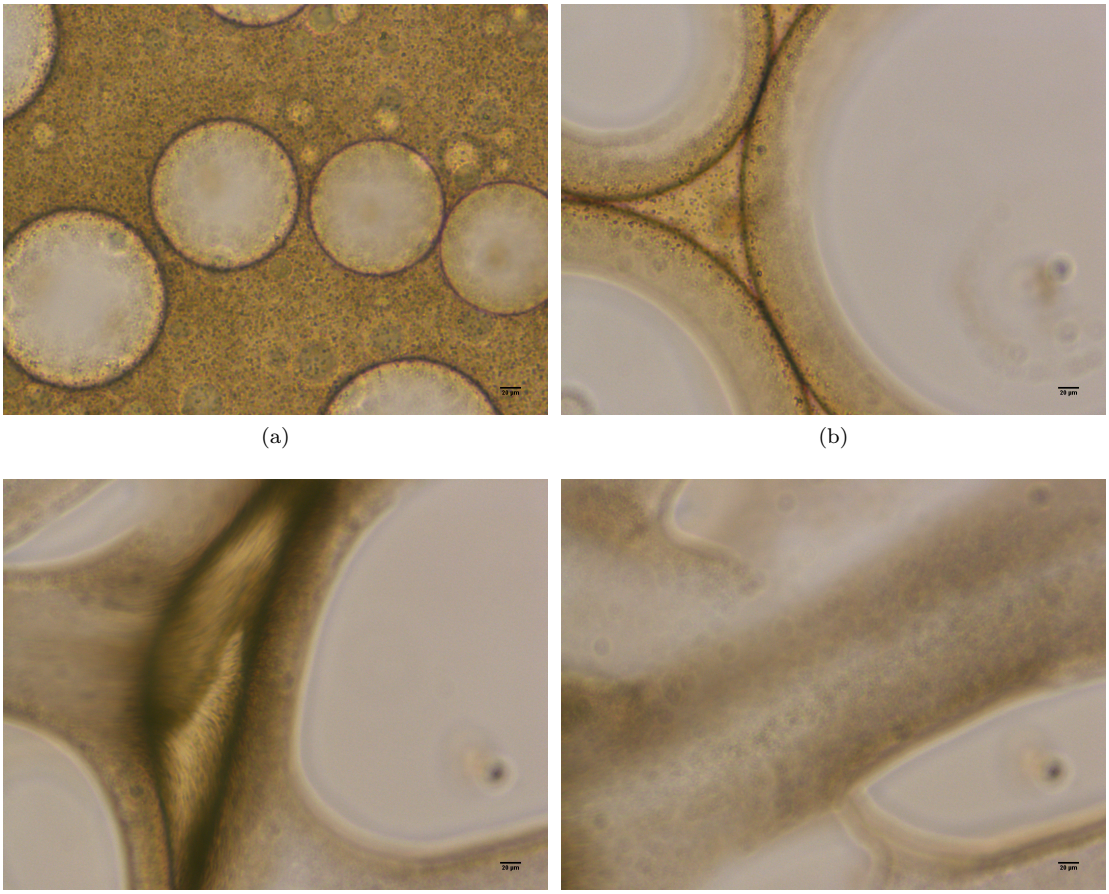

(a) (b)

(c) (d)

Figure 4.11: Diascopic microscopy images of temperature-controlled Pickering-like stabilization in a binary mixture of 31.7 wt% PnP and H_2O, dyed with fluorescein, with polystyrene colloids. a) The complete covering of droplets in a high concentration of colloids. b) At $\Delta T = 2.8\,°C$ Pickering-like stabilized droplets touch but do not coalesce for prolonged periods of time. c) Lowering the temperature to $\Delta T = 1.3\,°C$ causes detachment of the colloids from the interface and the loss of Pickering-like stability and droplets will coalesce . d) Finally, all three droplets have coalesced and the colloids adhered to the glass wall.

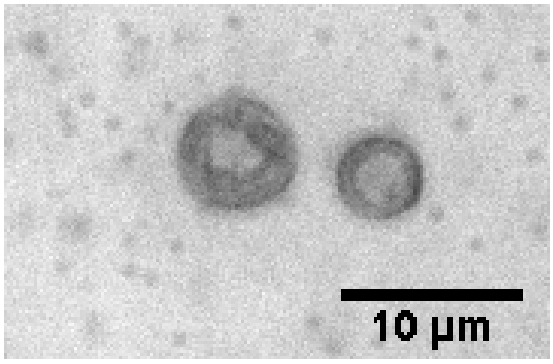

Figure 4.12: Episcopic microscopy images of aggregates of polystyrene particles formed in a binary mixture of 39.6 wt% PnP/H_2O after cooling a Pickering-like stabilized emulsion down to 4 °C below T_c. The particles covering the droplet form hollow colloidosome-like aggregates after the emulsion droplet has *evaporated*.

To obtain a reversible Pickering emulsion, polystyrene particles, which incorporated acryclic acid as a co-monomer (PSAA), were tested. The acrylic acid polymer brush acts as a steric stabilizer of the particles, preventing agglomeration. At sufficient high concentration these particles allowed a truly reversible Pickering stabilized emulsion as shown in fig. 4.13.

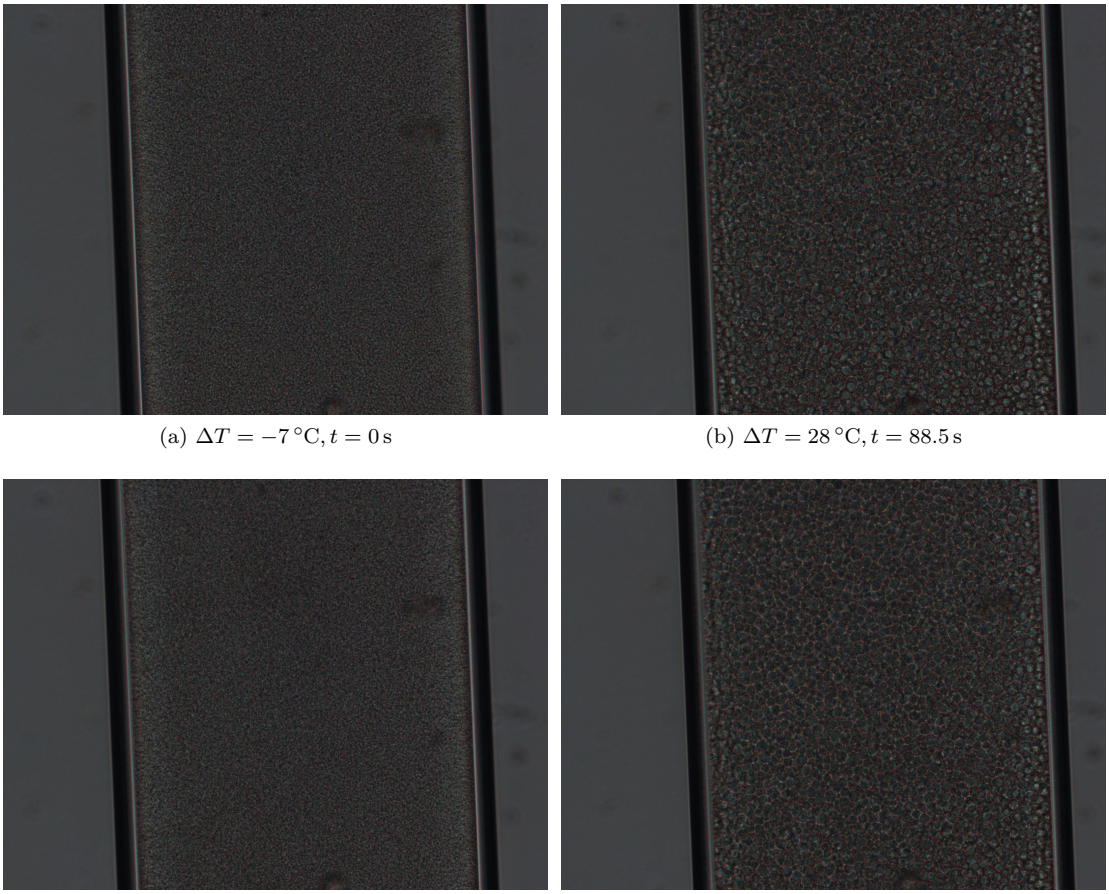

(a) $\Delta T = -7\,^{\circ}\mathrm{C}, t = 0\,\mathrm{s}$ (b) $\Delta T = 28\,^{\circ}\mathrm{C}, t = 88.5\,\mathrm{s}$

(c) $\Delta T = -7\,^{\circ}\mathrm{C}, t = 174.0\,\mathrm{s}$ (d) $\Delta T = 28\,^{\circ}\mathrm{C}, t = 286.5\,\mathrm{s}$

Figure 4.13: Diascopic microscopy images of temperature controlled Pickering-like stabilization of a binary mixture of 31.0 wt% PnP and H_2O, with PSAA colloids, studied in a capillary. a) High density of particles uniformly distributed through the capillary at room temperature. b) Pickering-like stabilized droplets after rapidly increasing the temperature, from 25 °C to 60 °C in 16.5 s, far above T_c. c) After cooling down to room temperature droplets disappear and particles are distributed uniformly, as in (a). d) Repeating the process of heating far above T_c leads to same result as in (b), showing the reversible nature.

At temperatures far above T_c, the particles adsorb to the interface and a stable emulsion is obtained. In contrast to the bare PS particles, these particles do not aggregate upon cooling down and thus the end situation is the same as the beginning. Repeating the heating and cooling cycle several times shows similar results. To check the possibility of stabilization by surfactants, particles were washed six times in a 30.2 wt% PnP/H_2O mixture. After washing, stable emulsions were observed upon heating, furthermore, a sample was taken from the supernatant of the centrifuged mixture, without any particles present, and stable emulsions were observed at $\Delta T = 28\,^{\circ}\mathrm{C}$. This leads to the assumption that surfactants are causing the stabilization and not the particles. Below $\Delta T = 2\,^{\circ}\mathrm{C}$, coalescence of droplets was observed in all studied PSAA systems, including the supernatant, indicating something not yet completely understood occurs at this temperature.

Just as for the PS particles, attraction of the particles was apparent and is shown in fig. 4.14. Different agglomeration *islands* could be seen on the droplets. Due to a weak inter-particle bond, particles did attach, move along the edge of these *islands*, and sometimes detach.

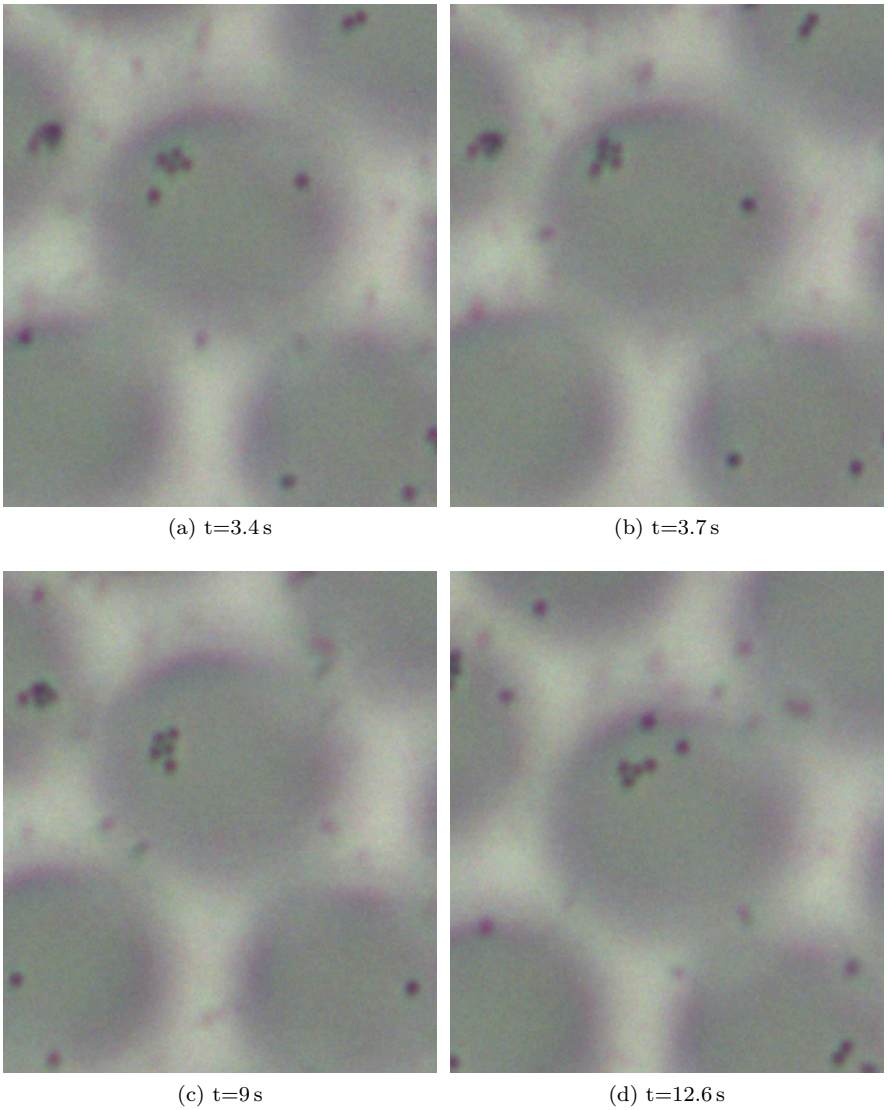

(a) t=3.4 s (b) t=3.7 s

(c) t=9 s (d) t=12.6 s

Figure 4.14: Diascopic microscopy images of reversible atrraction of poly(styrene-*co*-acrylic acid) acrylic acid copolymer colloids on the interface of a binary mixture of PnP/H_2O at $\Delta T = 28\,°C$. A particle can be seen that is free in (a), attached and moving along the surface of the *island* in (b,c), and detached again in (d).

4.6 Fluorescent colloids

Dye incorporated by swelling

PS colloids dyed with the swelling method, showed fluorescence and no leakage of the dye in water, although the signal was low. When adding these colloids to the binary mixture of PnP/H_2O dyed with fluorescein, no fluorescent particles were observed. It was concluded that the dye leaked out of the colloids since background emission was quite high. Probably the Rhodamin dye favours the binary mixture over the polystyrene interior of the particles. This method was thus not used for further measurements.

Covalently bound Dye

The dispersion of particles covalently successfully functionalized with fluorescein was studied using fluorescence microscopy (see fig. 4.15). However, upon combining the particles with a dye in the solution, Rhodamin B, fluorescence was not bright enough. Because non-functionalized particles could also be seen clearly, such particles were used for further measurements. Furthermore, this prevented effects of the polymer hairs and end groups on the behaviour of the system.

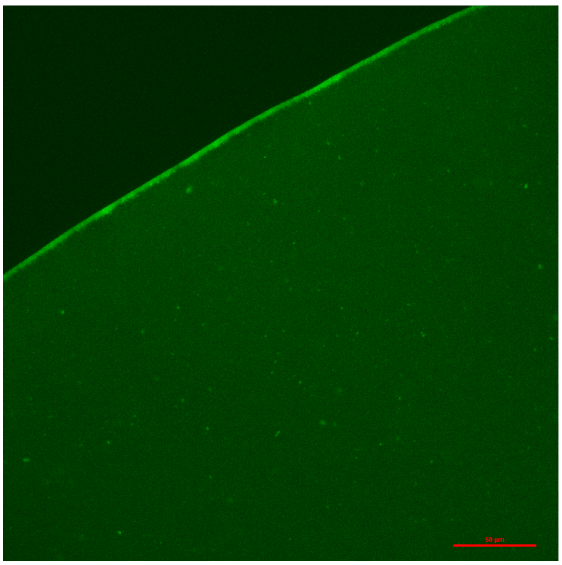

Figure 4.15: Episcopic microscopy image of fluorescent labelled PS colloids in H_2O. Contrast is slightly better than for non-functionalized particles but not greatly improved

Chapter 5

Conclusions

To conclude, we have shown that binary mixtures with a lower critical solution temperature (LCST) have a thermally tunable interfacial tension. The specific behaviour of two of these mixtures was studied, showing fading of the interface and increasing time for droplets to coalesce near the critical point. Interfacial tension tunability is shown by measuring the change of the contact angle of the dispersed phase with the glass. The effect of temperature on this contact angle, leads us to conclude that indeed the strength of the interfacial tension can be controlled by temperature. The change of apperent colloid adsorption to the interface upon temperature is also shown. It is also shown that at temperatures sufficiently close to T_c, the colloids reside at or near the interface for short times. This can be either caused by ultra-low interfacial tension or, more likely, other effects such as interface distortions or particles being driven close to the interface instead of adsorbing.

Furthermore, temperature-induced Pickering-like emulsions can be created that are only stable above a certain temperature. Below this temperature, particles move away from the interface, leading to coalescence of the emulsion droplets. These emulsions can be created just by heating, this in contrast to the laborious high shear methods currently in use.

To study this system a purpose-built heating set-up was used with a Peltier element and a heat reservoir allowing for uniform temperature fields in the x,y plane. The set-up allowed for temperature control of 0.1 °C, although temperature readouts are slightly unreliable during heating and cooling. Because of its size and shape it is easily adaptable to be used in alternative set-ups, such as heating a small flask, or using it in conjunction with a second heat source to create a non-uniform temperature.

Chapter 6

Outlook

To fully understand the system described in this thesis, several further studies should be considered. First of all, an accurate measurement of the interfacial tension dependence on temperature would be needed, either by the method of Grattoni et al. [17] or otherwise. This is a challenge because of the need to do the measurements of the interfacial tension and density at exact controlled temperatures. Conventional methods of measuring densities and interfacial tensions do not allow this with the set-up described in this thesis. A possibility is to use a thermostat environment. If these measurements exclude a hyper-low interfacial tension as the parameter responsible for desorption, other candidates should be investigated, such as temperature fluctuations or the possibility that the particles are not truly adsorbed at the interface. By looking at bigger particles, the precise position can possibly be observed. Another reason for desorption could be that it takes a long time for particles to reach their equilibrium contact angle. If the particles are pinned at a smaller contact angle, adsorption energies could be much lower than estimated in this thesis. This can be tested by allowing a sample to equilibrate longer before cooling.

Furthermore more insight is needed on the influence of a temperature gradient. This gradient is likely the cause of the toroidal flow we see around big droplets. Thermal gradients can also lead to interesting steady states by the thermophoresis of the particles and both solvents. Preliminary experiments show that phase separated droplets have a tendency to move in opposite direction of the particles.

Finally, to obtain thermo-reversible Pickering-like emulsions, particles need to be designed that can undergo the cooling of the system, and shrinking of the droplets, without aggregating. A first candidate for this would be particles with covalent bound steric stabilization chains. It is imperative to make absolutely sure that no surfactants are in the mixture to exclude surfactant stabilization. The polystyrene particles used in this study might be able to form more well-defined colloidosomes by better control of the heating and cooling rates. Fast heating and very slow cooling might provide lower polydispersity and a higher number of colloidosomes.

Chapter 7

Acknowledgements

I would like to thank Chris Evers for his daily supervision and learning me all the tricks of the microscope, and Willem Kegel for his supervision, great discussions and advice. Frans Dekker is thanked for providing the functionalized particles used for fluorescein labelling. Furthermore, I would like to acknowledge the Friday brainstorm sessions for great input and useful discussions. Finally I thank the entire FCC group and specifically the students that I shared an office with for a really great time.

Bibliography

[1] E. Cheluget, M. Weber, and J. Vera, "Modifications of the Flory-Huggins-Goldstein Model for Accurate Description of Closed-Loop Phase Diagrams," *Chemical Engineering Science*, vol. 48, no. 8, pp. 1415–1426, 1993.

[2] I. Nagata, M. Rogalski, and K. Miyamoto, "Correlation of binary coexistence curves of liquid-liquid equilibria over a wide temperature range using a new local composition model," *Thermochimica Acta*, vol. 224, pp. 59–69, 1993.

[3] M. D. Brown, B. M. Law, S. Satija, W. a. Hamilton, E. Watkins, J. H. J. Cho, and J. Majewski, "Comparison of critical adsorption scaling functions obtained from neutron reflectometry and ellipsometry," *Journal of Chemical Physics*, vol. 126, no. 20, pp. 1–9, 2007.

[4] V. D. Nguyen, S. Faber, Z. Hu, G. H. Wegdam, and P. Schall, "Controlling colloidal phase transitions with critical Casimir forces.," *Nature communications*, vol. 4, p. 1584, 2013.

[5] A. Gambassi, A. MacIolek, C. Hertlein, U. Nellen, L. Helden, C. Bechinger, and S. Dietrich, "Critical Casimir effect in classical binary liquid mixtures," *Physical Review E - Statistical, Nonlinear, and Soft Matter Physics*, vol. 80, no. 6, pp. 1–27, 2009.

[6] A. Oleinikova, L. Bulavin, and V. Pipich, "The Viscosity Anomaly Near the Lower Critical," *International Journal of Thermophysics*, vol. 20, no. 3, pp. 889–898, 1999.

[7] X. Song, Y. Pei, M. Qiao, F. Ma, H. Ren, and Q. Zhao, "Preparation and characterizations of Pickering emulsions stabilized by hydrophobic starch particles," *FOOD HYDROCOLLOIDS*, vol. 45, pp. 256–263, MAR 2015.

[8] C. Hudson, "The Reversible Solubility of Nicotine in Water," *Zeitschrift für Physikalische Chemie*, vol. 47, pp. 113–115, 1904.

[9] L. Almásy, *Structure and dynamics in binary mixtures with limited miscibility Investigation of aqueous solutions of methyl-substituted pyridines.* 2002.

[10] I. V. Brovchenko and A. V. Oleinikova, "Structural changes of the molecular complexes of pyridines with water and demixing phenomena in aqueous solutions," *The Journal of Chemical Physics*, vol. 106, no. 18, p. 7756, 1997.

[11] T. Narayanan and A. Kumar, "Reentrant phase transitions in multicomponent liquid mixtures," *Physics Reports*, vol. 249, no. 3, pp. 135–218, 1994.

[12] J. D. Cox, "897. phase relationships in the pyridine series. part ii. the miscibility of some pyridine homologues with deuterium oxide," *J. Chem. Soc.*, pp. 4606–4608, 1952.

[13] D. Subramanian, C. T. Boughter, J. B. Klauda, B. Hammouda, and M. a. Anisimov, "Mesoscale inhomogeneities in aqueous solutions of small amphiphilic molecules," *Faraday Discussions*, vol. 167, no. 0, pp. 217–238, 2013.

[14] H. Cox, W. Nelson, and L. Cretcher, "Correction. Reciprocal Solubility of the Normal Propyl Ethers of 1,2-Propylene Glycol and Water," *Journal of the American Chemical Society*, vol. 49, no. 12, p. 3189, 1927.

[15] K. Birdi, *Handbook of Surface and Colloid Chemistry, Third Edition.* 2009.

[16] R. Daniels, "Galenic principles of modern skin care products," 2001.

[17] C. A. Grattoni, R. A. Dawe, C. Y. Seah, and J. D. Gray, "Lower critical solution coexistence curve and physical properties (density, viscosity, surface tension, and interfacial tension) of 2,6-lutidine + water," *Journal of Chemical & engineering datahemical & engineering data*, vol. 38, no. 4, pp. 516–519, 1993.

[18] T. J. Seebeck, ""magnetische polarisation der metalle und erze durch temperatur-differenz" (magnetic polarization of metals and minerals by temperature differences)," *Abhandlungen der Kniglichen Akademie der Wissenschaften zu Berlin (Treatises of the Royal Academy of Sciences in Berlin)*, pp. 265–373, 1825.

[19] ""nouvelles expriences sur la caloricit des courants lectrique" (new experiments on the heat effects of electric currents),"

[20] O. Prucker, S. Christian, H. Bock, J. Ruhe, C. W. Frank, and W. Knoll, "On the glass transition in ultrathin polymer films of different molecular architecture," *Macromolecular Chemistry and Physics*, vol. 199, no. 7, pp. 1435–1444, 1998.

[21] M. L. Hair and W. Hertl, "Reaction of hexamethyldisilazane with silica.," *Journal of Physical Chemistry*, vol. 75, no. 14, pp. 2181–2185, 1971.

[22] C. H. J. Evers *et al.*, "Self-assembly of virus-like shells via colloidal bond hybridization and anisotropy," 2012, submitted.

[23] D. J. Kraft, *Model Systems for Self-Assembly.* 2010.

[24] F. Dekker, *Towards colloids for host-guest interactions.* 2015.